Automated Assessment of the Optic Nerve Head on Stereo Disc Photographs

Juan Xu,[1] *Hiroshi Ishikawa,*[1,2] *Gadi Wollstein,*[1] *Richard A. Bilonick,*[1] *Kyung R. Sung,*[1] *Larry Kagemann,*[1,2] *Kelly A. Townsend,*[1] *and Joel S. Schuman*[1,2]

Purpose. To develop automated software for optic nerve head (ONH) quantitative assessment from stereoscopic disc photographs and to evaluate its performance in comparison with human expert assessment.

Methods. A fully automated system, including three-dimensional ONH modeling, disc margin detection, cup margin detection, and calculation of stereometric ONH parameters, was developed and tested. One eye each from 54 subjects (23 healthy, 17 suspected glaucoma, and 14 glaucoma) was enrolled. The majority opinion of three experts defined disc and cup margins on the disc photographs was used for comparison. Seven ONH parameters, disc area, rim area, rim volume, cup area, cup volume, cup-to-disc (C/D) area ratio, and vertical C/D ratio, were computed based on both machine- and expert-defined margins and compared between the methods.

Results. All automated ONH measurements showed good correlation with the expert defined margins (Pearson $r = 0.90$, disc area; 0.56, rim area; 0.78, rim volume; 0.88, cup area; 0.93, cup volume; 0.69, C/D area ratio; and 0.67, vertical C/D ratio; all $P \leq 0.0001$). No statistically significant difference was found in the glaucoma-discriminating ability of all seven ONH parameters ($P \geq 0.21$). The mean or median of automatically defined disc and cup areas was significantly higher than the subjective assessment (disc area $P = 0.0001$, *t*-test; cup area $P = 0.036$, Wilcoxon signed ranks test), although they had high correlation coefficients. The software failed to detect the disc margin for all the disc photographs with peripapillary atrophy.

Conclusions. The automated ONH analysis method provides an objective and quantitative ONH evaluation using widely available stereo disc photographs. (*Invest Ophthalmol Vis Sci.* 2008;49:2512–2517) DOI:10.1167/iovs.07-1229

Glaucoma is the second most common cause of blindness worldwide, characterized by progressive damage of the optic nerve that may result in increasing visual field (VF) loss and eventual irreversible blindness.[1,2] Although ocular imaging instruments provide clinically useful quantitative assessment for glaucoma diagnosis and management, it is still the clinical standard to perform subjective optic disc assessment using ophthalmoscopy and disc photographs.

Stereo disc photography has been used to document structural abnormalities and longitudinal changes in glaucomatous eyes for decades. It is the most common widely used method for optic nerve head (ONH) imaging for analysis and diagnosis. Disc photographs are highly reproducible and record a natural color image of the retina.[2] One of the limitations of stereo disc photography, however, is that there is no fully automated ONH quantification method available. Conventional ONH evaluation includes estimation of the ONH dimensions by observing the image pair with a stereo viewer. Alternatively, computerized planimetry lets clinicians manually label the disc and cup margins and consequently generate several disc parameters.[3,4] This procedure is time consuming, labor intensive, and prone to high intra- and interobserver variability.[4,5]

In several studies, investigators used computerized methods for analyzing ONH structures, but these methods were all based on a single automated analysis technique, such as three-dimensional (3-D) ONH modeling[6–8] or disc margin detection,[9–16] and none of the studies integrated multiple techniques. Meanwhile, numerous techniques to identify the cup within 3-D topographic data have been proposed.[17–21] Previous studies have defined the top of the cup as 150 μm, 120 μm, one half, and one third of the distance posterior to the disc margin; all defined the bottom of the cup as the deepest point.[17–21] No gold standard criterion for the location of the anterior surface of the cup exists. We developed a fully automated system to perform ONH analysis from stereoscopic photographs using multiple-analysis methods that enabled the segmentation of all pixels in the image into disc, cup, and background regions based on the 3-D reconstructed model. The purpose of this study was to evaluate the glaucoma discriminating ability of the automated segmentation software of stereoscopic ONH photographs in comparison with human expert assessment.

Methods

Automated ONH Assessment System

The designed software generated 3-D ONH model and segment disc and cup so that various ONH parameters could be calculated automatically. Input into the system were pairs of stereo images taken from a conventional stereo camera. The analysis process included four steps: (1) 3-D ONH reconstruction, (2) disc margin detection, (3) cup margin detection, and (4) calculation of ONH stereometric parameters.

3-D ONH Reconstruction

In the stereo image pair, depth is inversely proportional to the disparity between the two matching points from the left and right images (Fig. 1), where the coordinate difference ($v_L - v_R$) of the corresponding points is defined as the disparity.[6,7] Multiple corresponding points

From the [1]UPMC Eye Center, Eye and Ear Institute, Ophthalmology and Visual Science Research Center, Department of Ophthalmology, University of Pittsburgh School of Medicine, Pittsburgh, Pennsylvania; and the [2]Department of Bioengineering, Swanson School of Engineering, University of Pittsburgh, Pittsburgh, Pennsylvania.

Supported in part by National Eye Institute Grant R01-EY13178-08; The Eye and Ear Foundation, Pittsburgh, PA; and an unrestricted grant from Research to Prevent Blindness, Inc., New York, NY.

Submitted for publication September 19, 2007; revised December 13, 2007, and January 28, 2008; accepted April 15, 2008.

Disclosure: **J. Xu**, None; **H. Ishikawa**, None; **G. Wollstein**, Carl Zeiss Meditec (F) and Optovue (F); **R.A. Bilonick**, None; **K.R. Sung**, None; **L. Kagemann**, None; **K.A. Townsend**, None; **J.S. Schuman**, Carl Zeiss Meditec (F, P, R) and Optovue (F, R)

The publication costs of this article were defrayed in part by page charge payment. This article must therefore be marked "*advertisement*" in accordance with 18 U.S.C. §1734 solely to indicate this fact.

Corresponding author: Hiroshi Ishikawa, UPMC Eye Center, Department of Ophthalmology, University of Pittsburgh School of Medicine, Eye and Ear Institute, 203 Lothrop Street, Pittsburgh, PA 15213; hii3@pitt.edu.

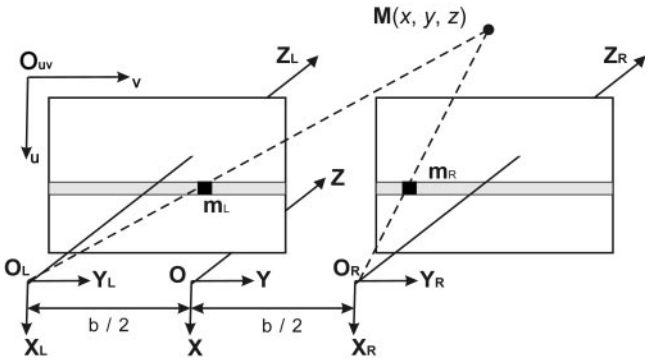

FIGURE 1. Parallel stereo image configuration.

were identified automatically on the left and right images by two matching methods: the highest correlation, and the minimum difference of features, where the features included the gradient magnitude, gradient orientation, and intensity. By measuring the cross-correlation and feature difference between the given comparison windows, we detected the corresponding points at the location with the highest correlation and the minimum difference. Only the corresponding points that were detected by both methods were used in the analysis, and the spatial disparities of the corresponding points were converted into depths. In the case of disagreement between the methods, depths were computed by interpolation from surrounding depths. A virtual 3-D ONH model was then generated from corresponding points and interpolation. The method of Xu et al.[8] was used to convert the virtually reconstructed 3-D ONH into an eye-specific model that accounted for the optical properties of each eye.

Disc Margin Detection

A deformable model technique was used to detect the disc margin, which included the following steps: locate the disc center, generate an initial contour, and deform to a final margin by minimizing an energy function defined from contour shape and contour location.

The region with the highest intensity on the image was located as the candidate region of optic disc. The edges of blood vessels and disc were detected to generate an edge map (Fig. 2). The initial disc margin and center were sought by searching a circle on the edge map near the candidate disc region, with the Hough transform technique.[22] This circular disc margin was refined by iteratively minimizing an energy function (deformable model technique) to detect a smooth boundary surrounding the disc center. The energy function was defined through the combined information from the intensity value, image gradient, and boundary smoothness.

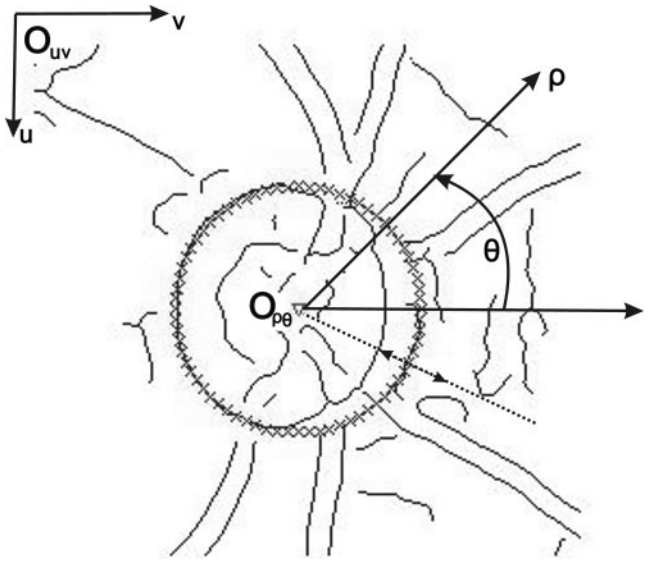

FIGURE 2. An example of initial disc margin on edge map. *Solid line*: blood vessel edges; (▽) initial disc center from the circle; ×, initial points of disc margin by searching a circle on the edge map; *arrowed line*: the deforming directions to refine the initial margin.

TABLE 1. Optic Nerve Head Parameter Definitions and Measurement Methods

	Definition	Unit
Disc area	Area inside the disc margin	mm^2 and/or pixels
Rim area	Area inside the disc margin but outside the cup margin	mm^2 and/or pixels
Rim volume	Number of voxels between the cup surface and the retinal surface	mm^3 and/or voxels
Cup area	Area inside the cup margin	mm^2 and/or pixels
Cup volume	Number of voxels inside the cup	mm^3 and/or voxels
C/D area ratio	Cup area divided by the disc area	
Vertical C/D ratio	Vertical cup diameter through the physical cup center divided by the disc diameter through the disc center	

Cup Margin Detection

An independent training set was used to determine the best cup definition, which was then tested on the current dataset. The cup margin was located 150 μm posterior to the disc margin for eyes with cup depths ranging between 0.2 and 1.0 mm. For eyes with cup depth shallower than 0.2 mm or deeper than 1.0 mm the cup margin was located at one fifth of the total depth. Smoothing of the cup margin was conducted by minimizing the energy function, similar to the technique just described, where the energy function incorporated depth information, location, gradient, smoothness, and shape.

Calculation of ONH Stereometric Parameters

Seven ONH parameters—disc area, rim area, rim volume, cup area, cup volume, cup-to-disc (C/D) area ratio, and vertical C/D ratio—were automatically generated by the software after applying the Littmann correction[23] for refraction and axial length. The definitions of the parameters appear in Table 1. An example of the consecutive steps of the automatic image processing is given in Figure 3.

Subjective Assessment of Stereo Photographs

Three glaucoma specialists manually defined the ONH and cup margins on the stereo disc photographs in a randomized masked fashion. The final location of the disc margin was defined by the majority opinion of the observers using the method described by Abramoff et al.[16] A similar procedure was used to define the location of the cup margin.

The same processes of 3-D reconstruction, depth calibration, and magnification correction methods were used on the stereo disc photographs that were labeled subjectively to generate sets of parameters identical with those generated automatically by the program.

Subjects and Image Acquisition

Fifty-four subjects recruited from the University of Pittsburgh Medical Center Eye Center (23 healthy, 17 suspected glaucoma, and 14 glaucoma) were enrolled to test the algorithm. Institutional Review Board (IRB) approval was obtained for the study, and all the patients gave

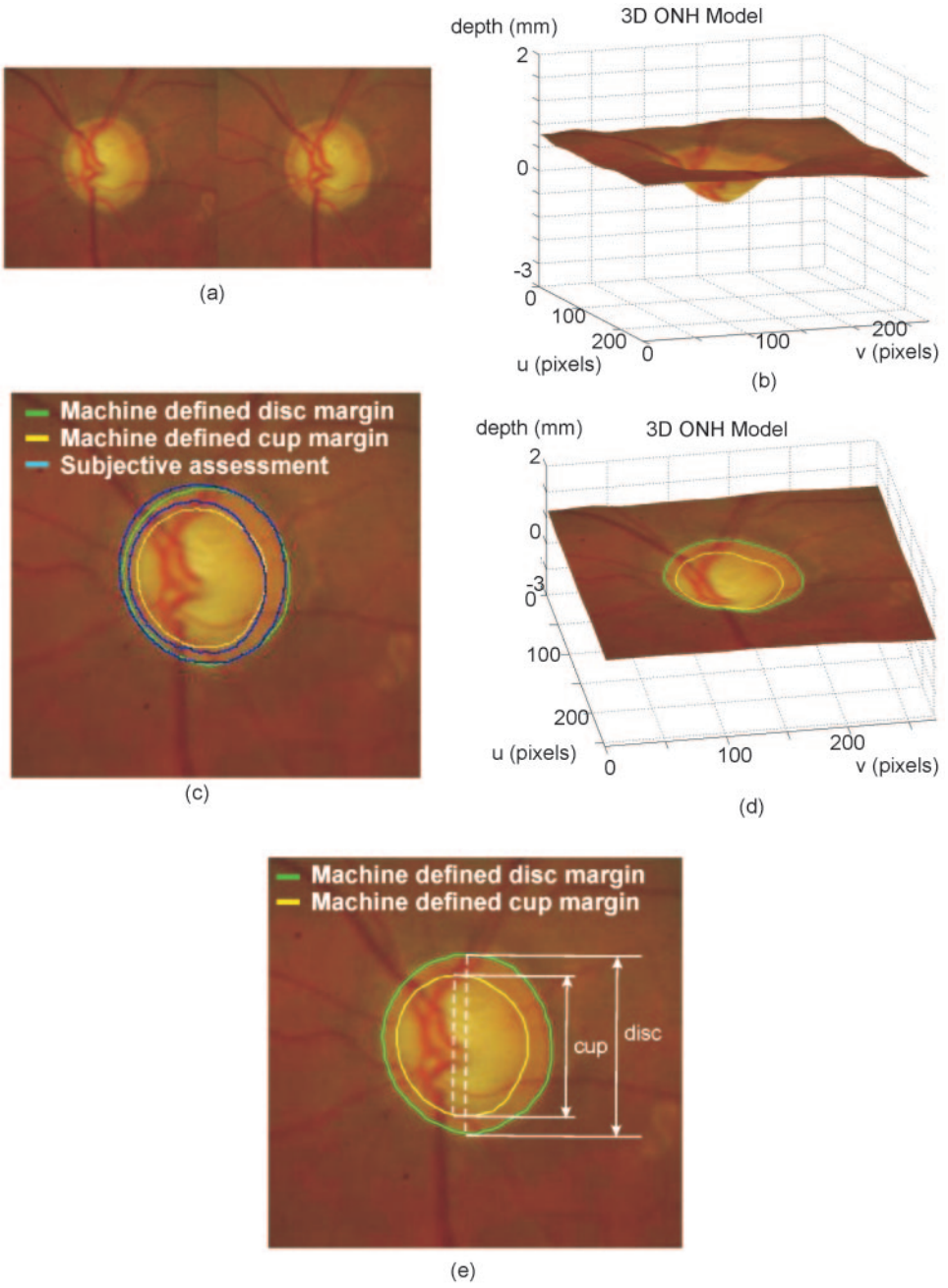

FIGURE 3. Automated optic nerve head (ONH) assessment system. (**a**) Stereo disc photograph, (**b**) 3-D ONH model after depth calibration, (**c**) computer-generated disc and cup margins on 2-D image, (**d**) computer-generated disc and cup margins on 3-D ONH model, and (**e**) ONH quantification.

their consent to participate. The study adhered to the Declaration of Helsinki and to Health Insurance Portability and Accountability Act regulations. All subjects had a comprehensive ophthalmic evaluation, reliable VF test results, and stereoscopic ONH photographs, all acquired within 6 months of each other. The evaluation included medical history, best corrected visual acuity, manifest refraction, intraocular pressure (IOP) measurements by Goldmann applanation tonometry, gonioscopy, slit lamp examination before and after pupil dilation, and VF testing. All subjects underwent pupillary dilation with 1% tropicamide and 2.5% phenylephrine (Alcon Laboratories, Fort Worth, TX).

The eye with the best quality disc photograph was selected from each patient if both eyes were eligible for the study. Stereo photographs were taken by simultaneous stereo fundus camera (model 3-Dx; Nidek, Fremont, CA) and digitized by a digital camera unit (D1x Nikon). The image resolution was 13,120 × 2,000 pixels. Axial length was measured in each eye (IOL master; Carl Zeiss Meditec, Dublin, CA). All subjects underwent Humphrey Swedish interactive thresholding algorithm standard or full-threshold 24-2 perimetry (Carl Zeiss Meditec). A reliable VF test was defined as one with fewer than 30% fixation losses or false-positive or -negative responses.

Eyes with Glaucoma or Suspected Glaucoma and Healthy Eyes

Eyes were defined as glaucomatous if both glaucomatous optic neuropathy (GON) and glaucomatous VF loss were present. GON was defined as intereye C/D ratio asymmetry >0.2, accounting for disc size; rim thinning or notching; C/D ratio ≥0.6; or disc hemorrhages. Glaucomatous VF loss was diagnosed if any of the following findings were evident on two consecutive VF tests: a glaucoma hemifield test outside normal limits, pattern SD (PSD) <5%, or a cluster of three or more nonedge points in typical glaucomatous locations (arcuate scotoma, nasal step, paracentral scotoma, or temporal wedge), all depressed on the pattern deviation plot at a level of $P < 0.05$, with one point in the

TABLE 2. Characteristics of the Study Participants

	Healthy (n = 23)	Glaucoma Suspect (n = 17)	Glaucoma (n = 14)	P
Age (y)	53.0 ± 9.0	55.7 ± 8.9	62.3 ± 8.9	0.01*
Male/female	6/17	4/13	3/11	0.88†
MD (dB)	−0.35 ± 5.57	−0.17 ± 1.52	−5.64 ± 5.57	<0.0001*

Values are means ± SD. MD, visual field mean deviation.
* ANOVA.
† χ^2 test.

cluster depressed at a level of $P < 0.01$. Eyes were defined as healthy if there was no history of glaucoma, IOP was ≤21 mm Hg, ONH did not meeting the criteria for GON as previously described, with a normal VF. Eyes with suspected glaucoma had no history of retinal disease, laser therapy, or intraocular surgery; IOP was 22 to 30 mm Hg and/or had asymmetric ONH cupping (difference in vertical C/D ratio greater than 0.2 between the eyes in the presence of similar optic disc sizes); increased cupping (vertical C/D ratio > 0.6 for average sizes ONH); or asymmetric cupping (>0.2 C/D diameter ratio difference between eyes), all in the presence of a normal VF test result.

Statistical Analysis

Failure of the software to detect the disc margin properly was defined as when the average distance between the automatically detected disc margin and the subjective assessed margin was larger than 5% (6 pixels) of the average disc diameter.

The results of the automated analysis of all eyes (including those defined as failure) were compared with the results of the subjective assessment by using Pearson correlation. The *t*-test was used to evaluate the differences in means between the automated and subjective assessments for disc area, C/D area ratio, and vertical C/D ratio, which have normal distributions, whereas the Wilcoxon signed ranks test was used to evaluate the differences in medians on all the other ONH parameters that had non-normal distributions (i.e., cup area, cup volume, rim area, and rim volume). Area under the receiver operating characteristic (AUC) curve was used to test the discrimination ability of each parameter in a subgroup that included only glaucomatous and healthy eyes (via the jackknife method[24] which is equivalent to the method of DeLong et al.[25]). $P < 0.05$ was considered statistically significant. The R Language and Environment for Statistical Computing[26] (R Development Core Team, 2007) was used for the statistical computations and graphics.

RESULTS

One eye of each of 54 subjects was enrolled to test the algorithms. The characteristics of the study participants are summarized in Table 2. Successful analysis was obtained from all tested photographs except for seven failures. Table 3 summarizes all seven generated parameters from the automated analysis and the subjective assessment for all subjects. All ONH measurements based on machine-defined margins showed a high correlation with the expert-defined margins. The mean or median of automatically defined disc and cup areas was significantly higher than the subjective assessment (disc area $P = 0.0001$, *t*-test; cup area $P = 0.036$, Wilcoxon signed-ranks test), although they had high correlation coefficients (disc area Pearson $r = 0.90$, cup area $r = 0.88$, both $P < 0.0001$). The measurements divided by the three subgroups are summarized in Table 4. Automated measurements of disc area of three subgroups and rim volume of the normal group were significantly higher than the subjective assessments. There was no statistically significant difference between the automated and subjective assessment for all other ONH parameters. A moderate to high correlation was observed for all parameters with the lowest correlation for rim area (Pearson's $r = 0.56$).

The discrimination ability of each parameter generated by the automated and subjectively assessed analysis is shown in Table 5. No statistically significant difference was found in glaucoma discriminating ability between machine- and human-defined margins for all the ONH measurements. The best automatically generated discriminatory parameter was cup volume (AUC = 0.85), and the worst was rim area (0.63).

DISCUSSION

In this study, we described a new method for automatically defining ONH parameters from stereoscopic disc photographs. There was no statistically significant difference in means or medians between automated and subjectively derived measurements for all the parameters except for disc and cup areas, with moderate to high correlation for all the parameters. Moreover, the discriminative ability of the methods was similar.

Disc area was significantly larger than the subjective measurement. This was mainly related to the presence of peripapillary atrophy that caused an overestimation by the automated

TABLE 3. Comparison of Optic Nerve Head Measurements Generated by Automated and Subjective Assessments for the Entire Subjects

	Automated Assessment*	Subjective Assessment*	P	Correlation Coefficient r§	P for r§
Disc area (mm^2)	2.61 ± 0.68	2.45 ± 0.60	0.0001† (−0.25, −0.08)	0.90	≤0.0001 (0.80, 0.94)
Rim area (mm^2)	1.50 ± 0.63	1.54 ± 0.37	0.33‡ (−0.15, 0.04)	0.56	≤0.0001 (0.26, 0.74)
Rim volume (mm^3)	0.26 ± 0.19	0.23 ± 0.16	0.071‡ (−0.07, 0.00)	0.78	≤0.0001 (0.66, 0.90)
Cup area (mm^2)	0.97 ± 0.57	0.76 ± 0.63	0.036‡ (−0.16, −0.01)	0.88	≤0.0001 (0.80, 0.94)
Cup volume (mm^3)	0.15 ± 0.26	0.16 ± 0.23	0.91‡ (−0.02, 0.02)	0.93	≤0.0001 (0.88, 0.97)
C/D area ratio	0.37 ± 0.16	0.36 ± 0.14	0.51† (−0.04, 0.02)	0.69	≤0.0001 (0.52, 0.85)
Vertical C/D ratio	0.61 ± 0.13	0.60 ± 0.12	0.29† (−0.04, 0.01)	0.67	≤0.0001 (0.50, 0.84)

* Mean ± SD for *t*-test; median ± interquintile range for Wilcoxon signed ranks test.
† *t*-Test (95% CI for mean difference).
‡ Wilcoxon signed ranks test (95% CI for median difference).
§ Pearson's correlation coefficient, P of r (95% CI for r).

TABLE 4. Comparison of Optic Nerve Head Measurements Generated by Automated and Subjective Assessments for Each Subgroup

	Normal			Glaucoma Suspect			Glaucoma		
	Automated Assessment*	Subjective Assessment*	*P*	Automated Assessment*	Subjective Assessment*	*P*	Automated Assessment*	Subjective Assessment*	*P*
Disc area (mm^2)	2.50 ± 0.46	2.32 ± 0.32	0.02† (−0.34, −0.03)	2.39 ± 0.50	2.27 ± 0.46	0.03† (−0.22, −0.02)	3.05 ± 0.96	2.86 ± 0.89	0.03† (−0.37, 0.02)
Rim area (mm^2)	1.58 ± 0.72	1.60 ± 0.40	0.52‡ (−0.22, 0.08)	1.41 ± 0.51	1.48 ± 0.37	0.82‡ (−0.15, 0.04)	1.45 ± 0.74	1.43 ± 0.41	0.29‡ (−0.46, 0.17)
Rim volume (mm^3)	0.33 ± 0.30	0.26 ± 0.23	0.01‡ (−0.16, −0.02)	0.21 ± 0.10	0.22 ± 0.07	0.82‡ (−0.09, 0.04)	0.20 ± 0.14	0.19 ± 0.18	0.95‡ (−0.07, 0.06)
Cup area (mm^2)	0.77 ± 0.50	0.71 ± 0.40	0.17‡ (−0.17, 0.03)	0.86 ± 0.34	0.76 ± 0.38	0.06‡ (−0.22, 0.02)	1.53 ± 0.82	1.44 ± 0.79	0.71‡ (−0.30, 0.17)
Cup volume (mm^3)	0.08 ± 0.15	0.12 ± 0.10	0.39‡ (−0.02, 0.03)	0.13 ± 0.18	0.15 ± 0.15	0.71‡ (−0.04, 0.06)	0.36 ± 0.30	0.34 ± 0.28	0.54‡ (−0.08, 0.04)
C/D area ratio	0.31 ± 0.13	0.29 ± 0.10	0.41† (−0.07, 0.03)	0.36 ± 0.11	0.34 ± 0.10	0.35† (−0.08, 0.03)	0.48 ± 0.19	0.50 ± 0.15	0.59† (−0.06, 0.10)
Vertical C/D ratio	0.57 ± 0.11	0.53 ± 0.09	0.13† (−0.08, 0.01)	0.61 ± 0.10	0.59 ± 0.09	0.55† (−0.07, 0.04)	0.69 ± 0.15	0.71 ± 0.12	0.54† (−0.04, 0.07)

* Mean ± SD for *t*-test, median ± interquintile range for Wilcoxon signed ranks test.
† *t*-Test (95% CI for mean difference).
‡ Wilcoxon signed ranks test (95% CI for median difference).

TABLE 5. Area under the Receiver Operating Characteristic Curve (95% CI) for Discriminating between Healthy and Glaucomatous Eyes

	AUC of Automated Assessment	AUC of Subjective Assessment	*P**
Disc area	0.68 (0.47–0.89)	0.66 (0.44–0.88)	0.66 (−0.08–0.12)
Rim area	0.63 (0.43–0.83)	0.74 (0.56–0.92)	0.25 (−0.29–0.08)
Rim volume	0.74 (0.57–0.91)	0.66 (0.48–0.85)	0.28 (−0.06–0.22)
Cup area	0.80 (0.61–1.00)	0.84 (0.68–1.00)	0.56 (−0.18–0.10)
Cup volume	0.85 (0.72–0.98)	0.85 (0.70–1.00)	0.93 (−0.07–0.07)
C/D area ratio	0.77 (0.59–0.96)	0.86 (0.72–1.00)	0.21 (−0.23–0.05)
Vertical C/D ratio	0.81 (0.64–0.98)	0.88 (0.74–1.00)	0.31 (−0.21–0.07)

* *P* of AUCs between automated and subjective assessments (95% CI for difference), jackknife estimator.[24]

analysis (Fig. 4). There were 7 disc photographs out of 54 with peripapillary atrophy, all leading to the failure of automated definition of disc margin. Because the location of the cup margin was dependent on the location of the disc margin, there was also a significant difference with this parameter. However, the differences in disc area and cup area were 0.16 mm^2 (mean difference) and 0.21 mm^2 (median difference, Table 3), respectively, which are of limited clinical significance. Rim area was dependent on both disc and cup margins. Therefore, the overdrawn margins did not directly affect the rim area, and there was no significant difference of rim area between the automated and subjective measurements. Similar results were observed when the data were analyzed separately for each clinical subgroup.

The rim area was relatively weakly correlated with the subjectively generated parameter (Table 3) and showed low discriminative ability (Table 5), probably because of the dependence of this parameter on the location of two margins (disc and cup margins), whereas disc and cup parameters were dependent on the position of a single margin. Although the cup margin of the automated program is dependent on the disc margin position, the subjective assessment of both the disc and the cup margin was independent.

FIGURE 4. An example of ill-defined disc and cup margins measured automatically, due to peripapillary atrophy.

Both rim and cup volumes showed better correlation between the automated and the subjectively defined measurements than the corresponding area parameters. This finding is related to the computational process of the 3-D parameters where both systems are using similar procedure and basic assumptions.

The automated software incorporates several predefined assumptions that improve the robustness and reliability of the algorithm. The cup margin location is directly related to the position of the disc margin, whereas the location is dynamically defined based on the dimension of the cup and thus accommodating for the wide anatomic varieties of the region. We assumed that the geometric disc center was located inside the cup contour. However, the accuracy of this algorithm may be reduced in cases of extreme shifts of cup location to one side of the disc. The software uses both the geometrical disc and cup centers for the calculation of the vertical C/D ratio. This ensures that, even in the presence of irregular contours or when the cup is shifted eccentrically, the ratio will be determined in the proper location.

Although we used a single stereo disc photograph system in this study, the automated software accepts stereo disc photograph images regardless of the model and make of the camera. The software requires the user to enter the following camera-specific parameters, to obtain the measurements: pixel size, image resolution, the baseline of the stereo lenses, and the view angle. Therefore the software is readily and widely applicable to daily clinical glaucoma assessment.

Searching the literature, we were able to find only one additional automated ONH analysis method of stereo photographs.[16] This method used a supervised machine classifier method that requires the use of a learning set whenever it is used. This is in contrast to the fully automated method we have described herein, which does not require the use of a testing set. Moreover, the method described by Abramoff et al.[16] provides 2-D measurements, whereas our method provides 3-D measurements such as rim and cup volumes.

In conclusion, our newly developed system showed potential to be useful for automated ONH assessment. It performed as well as human experts in glaucoma discrimination and ONH quantification. This may offer an effective option for ONH evaluation and longitudinal assessment by using the widely available stereo disc photographs.

References

1. Quigley HA. Number of people with glaucoma worldwide. *Br J Ophthalmol*. 1996;80:389–393.
2. Thylefors B, Negrel AD, Pararajasegaram R, Dadzie KY. Global data on blindness. *Bull World Health Organ*. 1995;73:115–121.
3. Sheen NJ, Morgan JE, Poulsen JL, North RV. Digital stereoscopic analysis of the optic disc: evaluation of a teaching program. *Ophthalmology*. 2004;111(10):1873–1879.
4. Eikelboom RH, Barry CJ, Jitskaia L, Voon ASP, Yogesan K. Neuroretinal rim measurement error using PC-based stereo software. *Clin Exp Ophthalmol*. 2000;28:178–180.
5. Garway-Heath DF, Poinoosawmy D, Wollstein G, et al. Inter- and intraobserver variation in the analysis of optic disc images: comparison of the Heidelberg retina tomograph and computer assisted planimetry. *Br J Ophthalmol*. 1999;83:664–669.
6. Deguchi K, Kawamata D, Mizutani K, Hontani H, Wakabayashi K. 3-D fundus shape reconstruction an display from stereo fundus images. *IEICE Trans Syst*. 2000;E83-D(7).
7. Corona E, Mitra S, Wilson M, Krile T, Kwon YH, Soliz P. Digital stereo image analyzer for generating automated 3-D measures of optic disc deformation in glaucoma. *IEEE Trans Med Imag*. 2002; 21(10):1244–1253.
8. Xu J, Chutatape O, Zheng C, Chew P. 3-D optic disc visualisation from stereo images via dual registration and ocular media optical correction. *Br J Ophthalmol*. 2006;90:181–185.
9. Osareh A, Mirmehdi M, Thomas B, Markham R. Comparison of colour spaces for optic disc localisation in retinal images. *Proceedings of the 16th International Conference on Pattern Recognition*. 2002;1(45):743–746.
10. Lowell J, Hunter A, Steel D, et al. Optic nerve head segmentation. *IEEE Trans Med Imag*. 2004;23(2):256–264.
11. Mendels F, Heneghan C, Thiran JP. Identification of the optic disc boundary in retinal images using active contours. *Proceedings of the IMVIP* [Irish Machine Vision and Image Processing] *Conference*. Dublin, Ireland: University of Dublin; 1999:103–115.
12. Li H, Chutatape O. Automated feature extraction in color retinal images by a model based approach. *IEEE Trans Biomed Engin*. 2004;51(2):246–254.
13. Lalonde M, Beaulieu M, Gagnon L. Fast and robust optic disc detection using pyramidal decomposition and Hausdorff-based template matching. *IEEE Trans Med Imag*. 2001;20(11):1193–1200.
14. Tamura S, Okamoto Y. Zero-crossing interval correction in tracing eye-fundus blood vessels. *Pattern Recog*. 1988;21(3):227–233.
15. Pinz A, Bernogger S, Datlinger P, Kruger A. Mapping the human retina. *IEEE Trans Med Imag*. 1998;17(4):606–619.
16. Abramoff MD, Alward WLM, Greenlee EC, et al. Automated segmentation of the optic disc from stereo color photographs using physiologically plausible features. *Invest Ophthalmol Vis Sci*. 2007;48:1665–1673.
17. Jaffe GJ, Caprioli J. Optical coherence tomography to detect and manage retinal disease and glaucoma. *Am J Ophthalmol*. 2004; 137:156–169.
18. Caprioli J, Klingbeil U, Sears M, Pope B. Reproducibility of optic disc measurements with computerized analysis of stereoscopic video images. *Arch Ophthalmol*. 1986;104(7):1035–1039.
19. Masunori K, Manabu N, Tsuguo N. A method for analyzing a stereoscopic image of a fundus, and an apparatus for executing that method. U.S. Patent no. EP0846439. June 1998.
20. Varma R, Spaeth GL. The PAR IS-2000: a new system for retinal digital image analysis. *Ophthalmic Surg*. 1988;19(3):183–192.
21. Hrynchak P, Hutchings N, Jones D, Simpson T. A comparison of cup-to-disc ratio measurement in normal subjects using optical coherence tomography image analysis of the optic nerve head and stereo fundus biomicroscopy. *Ophthalmic Physiol Opt*. 2004; 24(6):543–550.
22. Sonka M, Hlavac V, Boyle R. *Image Processing*, *Analysis*, *and Machine Vision.* Pacific Grove, CA: PWS Publishers; 1999.
23. Bennett AG, Rudnicka AR, Edgar DF. Improvements on Littmann's method of determining the size of retinal features by fundus photography. *Graefes Arch Clin Exp Ophthalmol*. 1994;232(6): 361–367.
24. Hanley JA, Hajian-Tilaki KO. Sampling variability of nonparametric estimates of the areas under receiver operating characteristic curves: an update. *Acad Radiol*. 1997;4:49–58.
25. DeLong ER, DeLong DM, Clarke-Pearson DL. Comparing the areas under two or more correlated receiver operating characteristic curves: a nonparametric approach. *Biometrics*. 1988;44:837–845.
26. R Development Core Team. R: A language and environment for statistical computing. R Foundation for Statistical Computing, Vienna, Austria; 2007 http://www.R-project.org.